Journal of Colloid and Interface Science 445 (2015) 119–126

Contents lists available at ScienceDirect

Journal of Colloid and Interface Science

www.elsevier.com/locate/jcis

N-methyldiethanolamine: A multifunctional structure-directing agent for the synthesis of SAPO and AlPO molecular sieves

Dehua Wang [a,b,c], Peng Tian [a,b], Dong Fan [a,b,c], Miao Yang [a,b], Beibei Gao [a,b,c], Yuyan Qiao [a,b,c], Chan Wang [a,b,c], Zhongmin Liu [a,b,*]

[a] National Engineering Laboratory for Methanol to Olefins, Dalian Institute of Chemical Physics, Chinese Academy of Sciences, Dalian 116023, PR China
[b] Dalian National Laboratory for Clean Energy, Dalian Institute of Chemical Physics, Chinese Academy of Sciences, Dalian 116023, PR China
[c] Graduate University of Chinese Academy of Sciences, Beijing 100049, PR China

GRAPHICAL ABSTRACT

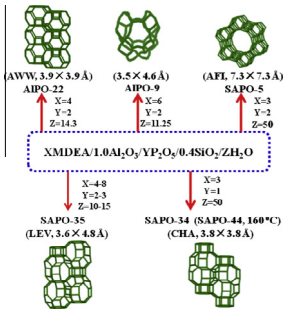

ARTICLE INFO

Article history:
Received 21 October 2014
Accepted 15 December 2014
Available online 24 December 2014

Keywords:
Alkanolamine
SAPO
Synthesis
Structure-directing agent
MTO reaction

ABSTRACT

In the present study, N-methyldiethanolamine (MDEA) is demonstrated to be a multifunctional structure-directing agent for the synthesis of aluminophosphate-based molecular sieves. Four types of molecular sieves, including SAPO-34, -35, AlPO-9 and -22, are for the first time acquired with MDEA as a novel template. The phase selectivity of the present synthesis is found to be condition-dependent. SAPO-34 (CHA) crystallizes from a conventional hydrothermal system with a higher MDEA concentration. When using MDEA as both the template and solvent, pure SAPO-35 (LEV) is obtained from the synthetic gel with a high P_2O_5/Al_2O_3 ratio of (2–3), in which the concentration of MDEA could be varied in a wide range. AlPO-9 and AlPO-22 (AWW) are synthesized under the similar conditions to SAPO-35, except without the addition of Si source. The physicochemical properties of the obtained samples are investigated by XRD, XRF, SEM, N_2 physisorption, TG-DSC, and various NMR spectra (^{13}C, ^{29}Si, ^{27}Al and ^{31}P). Both SAPO-34 and SAPO-35 show good thermal stability, large surface area, and high pore volume. The catalytic performance of SAPO-34 is evaluated by the methanol-to-olefins (MTO) reaction and a good ($C_2H_4 + C_3H_6$) selectivity of 82.7% has been achieved.

1. Introduction

Aluminophosphate (AlPO) molecular sieves were announced to be synthesized firstly by Union Carbide in the early 1980s [1,2]. Since then, many efforts have been stimulated to develop novel microporous AlPO materials by using hydro/solvo/ionothermal

* Corresponding author at: Dalian National Laboratory for Clean Energy, Dalian Institute of Chemical Physics, Chinese Academy of Sciences, Dalian 116023, PR China. Fax: +86 0411 84379998.
E-mail address: liuzm@dicp.ac.cn (Z. Liu).

http://dx.doi.org/10.1016/j.jcis.2014.12.029
0021-9797/

methods [3–5]. In addition, multiple compositions of AlPO based molecular sieves such as silicoaluminophosphates (SAPOs) [6–8] and metal-substituted aluminophosphates (MeAPOs) [9,10] have been prepared. The successful synthesis of such materials is generally condition dependent, referring to the synthetic parameter including the nature and relative ratios of source materials in the initial gel, the heating temperature and the heating time. Among these parameters, the template or structure-directing agent (SDA) is thought to be the most important factor [11,12]. However, it must be noted that gel chemistry is also crucial [13], and that the templating action will not function well unless the correct gel environment is achieved. For example, Yan et al. have made detailed investigation on this important issue recently. They found that the concentration of the chemicals can affect the formation of intermediate phase in the crystallization pathway of AlPO-11 [14]. Also the relative ratios of species and crystallization temperature can affect the structure-directing ability of the organic amines, leading to different products [15,16].

For SAPO synthesis, the employment of organic additives as SDA or template in the synthetic gel is indispensable. These organic additives are essential for the organization of the TO_4 units into the ordered crystalline structure [17,18]. Although the detailed functional mechanism of these templates is still far from clarity, it is generally acknowledged that they are encapsulated into the synthesized crystalline materials and stabilize the frameworks via a combined van der walls and electrostatic interactions [17,19]. However, the so-called *template effect* might not be so specific as one expect. A case in point is the one template/multiphase phenomenon. For example, dipropylamine (DPA) as one of the simplest amines have been demonstrated to be able to direct the synthesis of at least 10 different structure types of microporous materials [20,21]. Another example is the multiple template/single phase phenomenon, as evidenced by SAPO-34 synthesis. Specifically, many kinds of organic amines have been found to be capable of directing SAPO-34 molecular sieves, including tetraethylammonium hydroxide (TEAOH) [22], dipropylamine [7], isopropylamine [23], piperidine [24], morpholine (MOR) [25], triethylamine (TEA) [26], and diethylamine (DEA) [27,28], etc. The distinction of elemental compositions, morphology as well as local microscopic structure might exist for a specific molecular sieve synthesized with different templates, which further influences the catalytic performances and adsorption properties of the obtained products. For instance, it has been reported that TEAOH is capable to direct the synthesis of SAPO-34 nano-crystals with long lifetime and high selectivity to light olefins in the MTO reaction [22,29,30], while both MOR and DEA tend to direct the synthesis of micron-sized SAPO-34 crystals with high Si incorporation into the framework [25,27]. Barthomeuf et al. have made a detailed investigation into the relationship between the template and the Si environments of SAPO-34, concluding that the template could determine the maximum charge and govern the Si distribution and thus the acidity of the molecular sieve [11].

Alkanolamines, as a class of organic amines have been paid little attention for molecular sieve synthesis in the past years and the corresponding research about the physicochemical properties of the obtained molecular sieves is scarce [31]. Compared with alkylamines, alkanolamines have higher boiling point, alleviating safety concerns with relatively low pressure during the crystallization process. Moreover, alkanolamines possess stronger polarity and better compatibility with water due to the existence of hydroxyl groups in the molecule structure [32]. Recently, employing alkanolamines as both the solvent and template, we have managed to synthesize some novel SAPO molecular sieves with special properties and performances. Diglycolaime (DGA) and diisopropanolamine (DIPA) were proved to be effective templates for SAPO-34 synthesis for the first time and SAPO-34 synthesized with DGA template exhibits large CO_2 adsorption capacity and high CO_2-over-CH_4 selectivity [33].

N-methyldiethanolamine, having similar molecule size to dipropylamine, remains less explored as template for the synthesis of molecular sieves. It is speculated that MDEA might also be a multifunctional template for aluminophosphate based molecular sieves. Herein, a thorough investigation into the synthesis of SAPO and AlPO molecular sieves using MDEA as the template and/or solvent have been carried out. Interestingly, by adjusting the synthetic variables, several SAPO/AlPO molecular sieves with different structures were obtained with MDEA as a novel template.

2. Experimental section

2.1. Sample preparation

N-methyldiethanolamine (MDEA) used in the synthesis was analytically reagent. Silica sol (31 wt%), pseudoboehmite (72.5 wt%) and phosphoric acid (85 wt%) were used as inorganic reactants.

A typical synthesis procedure was as follows: N-methyldiethanolamine, water, pseudoboehmite and silica sol were added in sequence into a glass beaker. The mixture was stirred at room temperature for 10 min, and then transferred into a stainless steel autoclave. Subsequently the phosphoric acid was added into the mixture drop by drop with stirring and a homogeneous and viscous mixture was obtained, following which the autoclave was sealed and placed in an oven. After the autoclave being rotated at 50 rpm for 30 min to get a more homogeneous mixture, it was heated under autogenous pressure at a certain temperature under rotation and kept for a certain time. At the end of the crystallization, the products were recovered by filtration with distilled water, and dried at 100 °C in air. As-synthesized materials were calcined in air at 550 °C for 4 h to obtain the template-free samples.

2.2. Characterizations

The powder XRD patterns were recorded on a PANalytical X'Pert PRO X-ray diffractometer with Cu Kα radiation (λ = 1.54059 Å), operating at 40 kV and 40 mA. The chemical composition of the samples was determined with Philips Magix-601 X-ray fluorescence (XRF) spectrometer. The crystal morphology was observed by field emission scanning electron microscopy (Hitachi, SU8020). All the solid state NMR experiments were performed on a Bruker AvanceIII 600 spectrometer equipped with a 14.1 T wide-bore magnet. The resonance frequencies were 150.9, 156.4, 242.9 and 119.2 MHz for ^{13}C, ^{27}Al, ^{31}P and ^{29}Si, respectively. ^{13}C CP MAS, ^{27}Al and ^{31}P MAS NMR experiments were performed on a 4 mm MAS probe with a spinning rate of 12 kHz. ^{13}C CP NMR spectra were recorded with a contact time of 3 ms and a recycle delay of 2 s. ^{27}Al MAS NMR spectra were recorded using one pulse sequence. A 200 scans were accumulated with a $\pi/8$ pulse width of 0.75 μs and a 2 s recycle delay. Chemical shifts were referenced to $(NH_4)Al(SO_4)_2{\cdot}12H_2O$ at −0.4 ppm. ^{31}P MAS NMR spectra were recorded using high-power proton decoupling. A 32 scans were accumulated with a $\pi/4$ pulse width of 2.25 μs and a 10 s recycle delay. Chemical shifts were referenced to 85% H_3PO_4 at 0 ppm. ^{29}Si MAS NMR spectra were recorded with a 7 mm MAS probe with a spinning rate of 6 kHz using high-power proton decoupling. A 5000–6000 scans were accumulated with a $\pi/4$ pulse width of 2.5 μs and a 10 s recycle delay. Chemical shifts were referenced to 4,4-dimethyl-4-silapentane sulfonate sodium salt (DSS). N_2 adsorption–desorption isotherms were obtained on a Micrometrics ASAP 2020 system at 77 K. The total surface area was calculated based on the BET equation. The micropore volume and micropore

Table 1
The influence of synthetic parameters on the synthesis results based on the MDEA system.

Sample	Gel composition MDEA:Al_2O_3:P_2O_5:SiO_2:H_2O	$V_{amine/water}$	T (°C)	t (h)	Product	Product composition	Si [a] incorporation
1	1.0: 1.0: 1.0: 0.4: 50		200	48	SAPO-34 + SAPO-5		
2	3.0: 1.0: 1.0: 0: 50		200	48	Amorphous		
3	3.0: 1.0: 1.0: 0.2: 50		200	48	SAPO-34	$Al_{0.499}$ $P_{0.393}$ $Si_{0.108}$	2.29
4	3.0: 1.0: 1.0: 0.4: 50		200	48	SAPO-34	$Al_{0.465}$ $P_{0.409}$ $Si_{0.136}$	1.49
5	3.0: 1.0: 1.0: 0.75: 50		200	48	SAPO-34	$Al_{0.471}$ $P_{0.353}$ $Si_{0.176}$	1.11
6	3.0: 1.0: 1.0: 1.0: 50		200	48	SAPO-34 + amorphous SiO_2	$Al_{0.458}$ $P_{0.360}$ $Si_{0.182}$	0.91
7	3.0: 1.0: 1.0: 0.75: 50		160	48	SAPO-44	$Al_{0.496}$ $P_{0.365}$ $Si_{0.139}$	0.88
8	3.0: 1.0: 2.0: 0.4: 50		200	48	SAPO-5		
9	4.0: 1.0: 2.0: 0.4: 14.3	1.8	200	48	SAPO-35	$Al_{0.472}$ $P_{0.453}Si_{0.075}$	1.21
10	6.0: 1.0: 2.0: 0.4: 11.25	3.4	200	48	SAPO-35	$Al_{0.475}$ $P_{0.440}$ $Si_{0.085}$	1.41
11	8.0: 1.0: 2.0: 0.4: 15	3.4	200	48	SAPO-35	$Al_{0.476}$ $P_{0.428}Si_{0.098}$	1.58
12	8.0: 1.0: 3.0: 0.4: 15	3.4	200	48	SAPO-35		
13	8.0: 1.0: 1.0: 0.4: 15	3.4	200	17	SAPO-44	$Al_{0.484}$ $P_{0.389}$ $Si_{0.127}$	1.43
14	6.0: 1.0: 2.0: 0.2: 11.25	3.4	200	48	Amorphous		
15	6.0: 1.0: 2.0: 0.75: 11.25	3.4	200	48	SAPO-35	$Al_{0.478}$ $P_{0.428}$ $Si_{0.094}$	0.87
16	6.0: 1.0: 2.0: 1.0: 13.4	3.4	200	48	SAPO-35	$Al_{0.477}$ $P_{0.417}$ $Si_{0.106}$	0.77
17	6.0: 1.0: 2.0: 0: 11.25	3.4	200	48	AlPO-9		
18	4.0: 1.0: 2.0: 0: 14.3	1.8	200	36	AlPO-22		

[a] Si incorporation = $[Si/(Si + Al + P)]_{product}/[Si/(Si + Al + P)]_{gel}$.

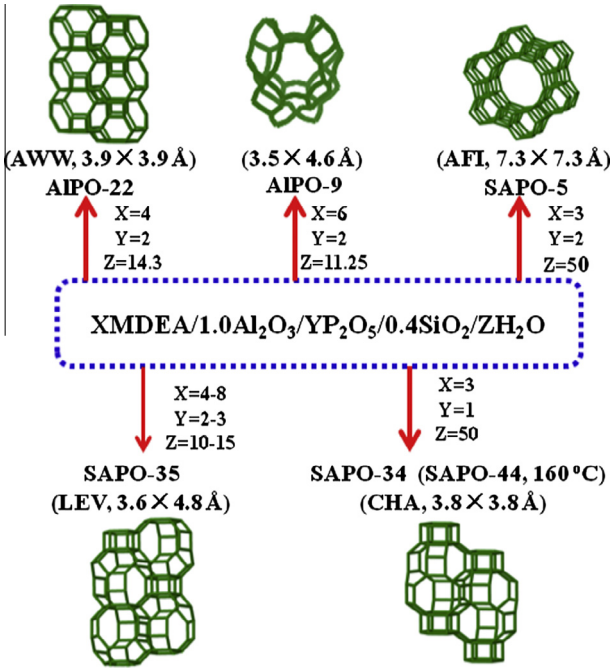

Fig. 1. Synthetic results with MDEA as the template. The framework structure, pore size, and structure code of each product are also illustrated in the figure.

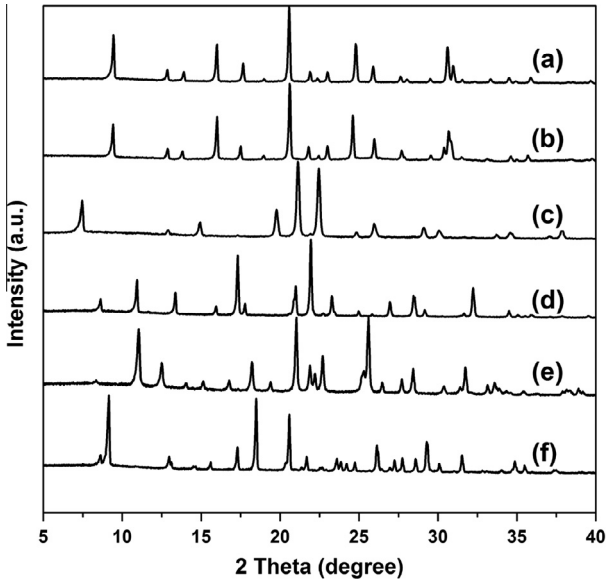

Fig. 2. XRD patterns of the as-synthesized samples 4 (a), 7 (b), 8 (c), 10 (d), 17 (e) and 18 (f).

surface area were evacuated using the t-plot method. The thermal analysis was performed on a TAQ-600 analyzer with a temperature-programmed rate of 10 °C/min under an air flow of 100 ml/min.

2.3. Catalyst evaluation

Methanol to olefins (MTO) reactions was performed in a quartz tubular fixed-bed reactor at atmospheric pressure. 0.3 g of the calcined sample (40–60 mesh) were loaded into the reactor. The catalyst loaded in the quartz reactor was activated at 550 °C in a He flow of 30 ml/min for 1 h before starting each reaction run, and then the temperature was adjusted to a reaction temperature of 450 °C. The methanol was fed by passing the carrier gas (42 ml/min) through a saturator containing methanol at 23 °C, which gave a WHSV of 2.0 h^{-1}. The reaction products were analyzed using an online gas chromatograph (Agilent GC 7890N), equipped with a flame ionization detector (FID) and Plot-Q column.

3. Results and discussion

3.1. Synthesis of SAPO and AlPO molecular sieves with MDEA as the template

The results of representative syntheses with MDEA as the template are summarized in Table 1, including gel compositions, product phases and inorganic elemental analyses of selected samples. Under the conventional hydrothermal conditions (xMDEA/$1Al_2O_3/1P_2O_5/0.4SiO_2/50H_2O$), lower MDEA dosage (MDEA/Al_2O_3 = 1) only yield a mixed product of SAPO-5 and SAPO-34 (sample 1) after 2 days of crystallization at 200 °C. By increasing the MDEA/P_2O_5 ratio to 3, SAPO-34 (sample 4) could be readily acquired. This is in agreement with the previous reports that

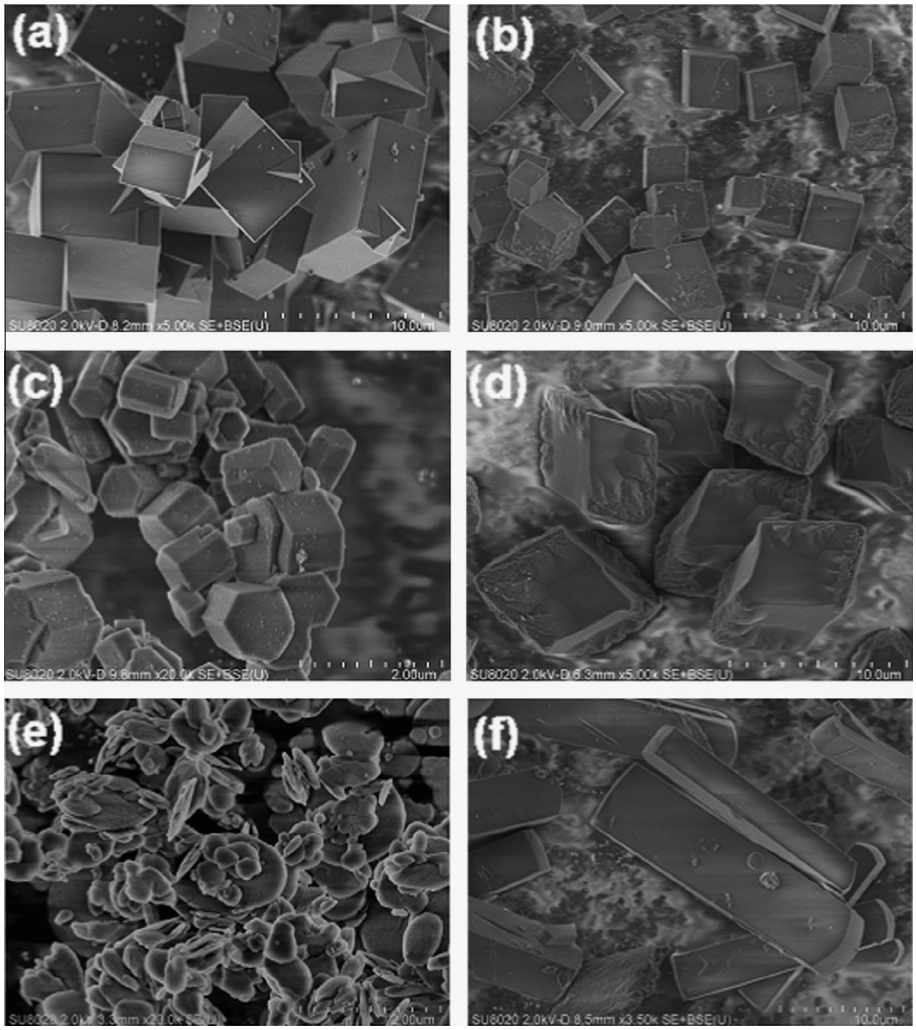

Fig. 3. SEM images of as-synthesized samples 4 (a), 7 (b), 8 (c), 10 (d) and 17 (e) and 18 (f).

Table 2
Textual properties of SAPO-34 (sample 4) and SAPO-35 (sample 10).

Sample	Surface area (m^2/g)			Pore volume (cm^3/g)	
	S_{total} [a]	S_{micro} [b]	S_{ext} [c]	V_{total}	V_{micro} [d]
4	555	555	0	0.27	0.27
10	539	515	24	0.25	0.24

[a] BET surface area.
[b] t-plot micropore surface area.
[c] t-plot external surface area.
[d] t-plot micropore volume.

increasing the gel alkalinity is better for the formation of pure phase of SAPO-34. In addition, SAPO-44 (sample 7) may also be obtained by carrying out the crystallization of the initial gel of sample 5 at 160 °C. This result is not very surprising considering that both SAPO-34 and SAPO-44 possess the same chabazite structure topology, though some structure distortion exists in the framework of the latter [34].

When changing the H_3PO_4 amount in the initial gel to $P_2O_5/Al_2O_3 = 2$, more interesting results are observed. Pure SAPO-5 crystallized from a staring molar composition of $3MDEA/1Al_2O_3/2P_2O_5/0.4SiO_2/50H_2O$. By further increasing the MDEA amount and lowering the water concentration in the gel, another type of molecular sieve SAPO-35 (samples 9–12) could be obtained. From Table 1, the Si concentration in SAPO-35 product rises with the increasing

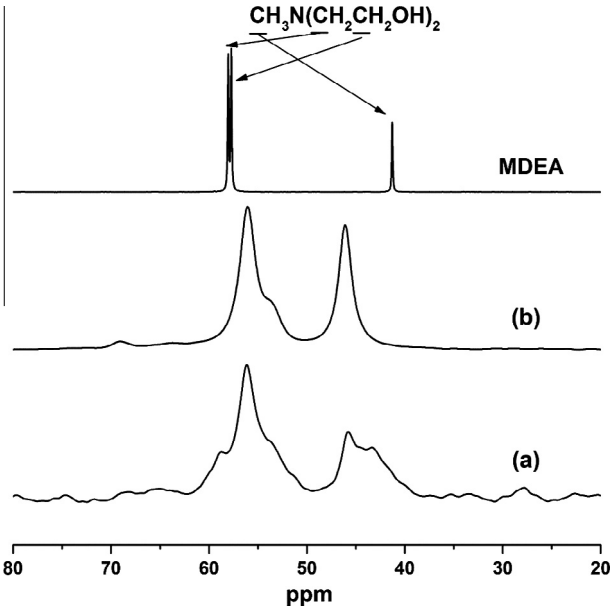

Fig. 4. ^{13}C CP MAS NMR spectra of the as-synthesized samples 4 (a) and 10 (b). ^{13}C NMR spectrum of the MDEA resource is shown in the figure as a comparison.

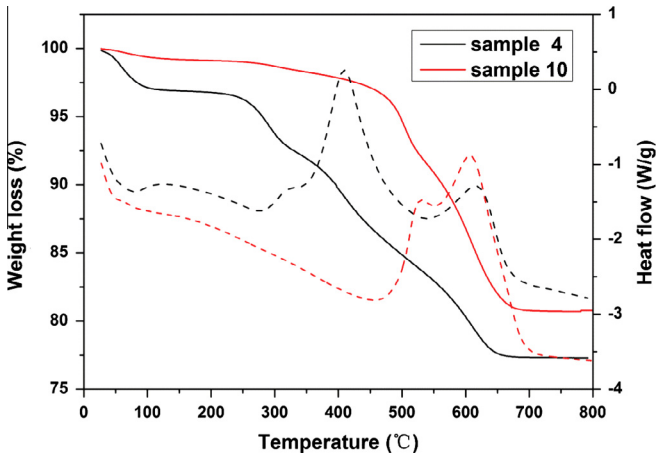

Fig. 5. TG (solid line) and DSC (dash line) curves of the as-synthesized samples SAPO-34 (sample 4) and SAPO-35 (sample 10).

MDEA concentration in the gel, suggesting that higher template amount benefit the incorporation of silicon into the framework. The synthetic gel for SAPO-35 is in fact an aminothermal environment because the MDEA/H_2O volume ratio reaches 1.8–3.4, in which MDEA can be considered as both the solvent and template. It should be mentioned that higher P_2O_5/Al_2O_3 ratio in the starting gel is crucial for the successful synthesis of SAPO-35. If the ratio is reduced to 1, the synthetic product would change to SAPO-44 (sample 13). Furthermore, two types of AlPO molecular sieves AlPO-9 (sample 17) and AlPO-22 (sample 18) may also be synthesized if there is no Si source in the synthetic systems of SAPO-35. AlPO-9 and -22 was first reported by Wilson et al. in a patent with 1,4-diazabicyclo (2.2.2) octane (DABCO) and N,N′-dimethyl-l,4diazabicyclo (2,2,2) octane dihydroxide (DDO) as the SDA, respectively [2]. In 2001, Xu et al. determined the structure of AlPO-9 by using both piperazine (detonated as AlPO-CJ11) [35] and hexamethylenetetramine (detonated as AlPO-CJB2) [36] as the SDA. Recently, Ding et al. also reported the synthesis and structure of AlPO-9 with the presence of piperazine [37]. Regarding AlPO-22, Richardson once investigated the crystal structure of AlPO-22 with quinuclidine as the SDA [38], and found that there is one phosphate group (HPO_4^{2-}) trapped in each cavity of the framework. Later, Yan et al. reported the single-crystal X-ray structural analysis of this material (a new name of AlPO-CJB-1 was assigned) template by hexamethylenetetramine. The position of phosphate group in the cage was also clearly determined [39].

From the above results, MDEA is a multifunctional SDA which could direct the synthesis of six types of molecular sieves (SAPO-5, -34, -35, -44, AlPO-9 and -22) with pore sizes changing from 8- to 12-membered rings. The topology structures of each product, showing the channels and apertures, are illustrated in Fig. 1. Among them, SAPO-44 was reported by us recently via aminothermal synthesis with MDEA as the SDA (sample 13). AlPO-5 was also patented to be prepared hydrothermally using MDEA as the SDA [2]. To the best of our knowledge, this is the first synthesis report of SAPO-34, -35, AlPO-9 and -22 templated by MDEA. Although a rational relationship between the structure and synthesis condition cannot be established through the present results, it is clear that the structure-directing effect of MDEA is really condition dependent, which can be notably altered by the organic concentration in synthesis mixtures, the P_2O_5/Al_2O_3 ratios, and the introduction of Si source. At present, much attention has been put to the design and synthesis of novel template molecules in order to synthesize molecular sieves with novel structures/compositions or special morphologies. The present results indicate that varying the synthetic parameters based on the conventional amine systems may also give the possibility to obtain interesting results.

The power XRD patterns of the selected samples are displayed in Fig. 2. All of them are comparable to those reported in the previous literatures, confirming the phase purity of each molecular sieve. The major difference in the XRD patterns of SAPO-34 and SAPO-44 exists in the distance of two peaks in the range of 23–26° (2θ) and the relative intensities of the neighboring peaks around 30° (2θ).

The morphological features of the samples are shown in Fig. 3. Hexagonal prism morphology with crystal size of 0.4–1 μm is observed for SAPO-5. Both SAPO-34 and SAPO-44 show a typical rhombohedral morphology with crystal size of 3–5 μm. The difference observed between these two materials is the presence of twinning in SAPO-34. SAPO-35 crystals also presents rhombohedral shape, but with uneven surface. The crystal size of SAPO-35 is around 6 μm. Dics-like crystals are observed with AlPO-9, which diameter ranges from 0.3 to 1 μm. AlPO-22 displays slab-like morphology with relatively large crystal size of 14 μm in length and ~4 μm in width.

3.2. Effect of Si content on the synthesis of SAPO-34 and SAPO-35

It is well known that the silicon content has great influence on the acidity and catalytic property of SAPO molecular sieves. A detailed research about the effect of silicon content on the synthesis of SAPO-34 and -35 was thus carried out. The results are displayed in Table 1. The elemental compositions of the final products determined by XRF are also given in Table 1. Without Si in the initial gel for the synthesis of SAPO-34, only amorphous product was observed. Pure SAPO-34 could be obtained when the SiO_2 content is kept in the range of $0.2 \leqslant SiO_2/Al_2O_3 \leqslant 0.75$. Further increasing the Si content to 1.0, a small amount of amorphous phase due to the unreacted silica residues started to appear in the product, implying the capacity limitation of silicon incorporation into the framework of SAPO-34. The Si concentration in the SAPO-34 products rises with its increase in the gel, though the Si incorporation degree shows a decreasing trend. For SAPO-35, amorphous products were obtained if the SiO_2 content in the initial gel was less than 0.2 (SiO_2/Al_2O_3 ratio). By increasing the Si content to 0.4 or higher, pure SAPO-35 could be readily synthesized. The silicon concentration in SAPO-35 also shows an increasing trend following its addition in the gel, but the variation range is relatively narrow as compared to that of SAPO-34.

3.3. Physiochemical properties of the samples: N_2 physisorption, ^{13}C MAS NMR, TG-DSC, ^{29}Si, ^{27}Al and ^{31}P MAS NMR

Among the four molecular sieves synthesized with MDEA as a novel template, AlPO-9 is thermally unstable, which lose its

Table 3
Thermal analysis results of SAPO-34 (sample 4) and SAPO-35 (sample 10).

Sample	Weight loss (%)				T atom per cage	Template number per cage
	I	II	III	IV		
4	3.3 (<210 °C)	3.9 (210–320 °C)	8.3 (320–510 °C)	6.9 (510–650 °C)	12	1.54
10	1.3 (<300 °C)	1.6 (300–450 °C)	2.4 (450–500 °C)	13.3 (500–660 °C)	9	1.05

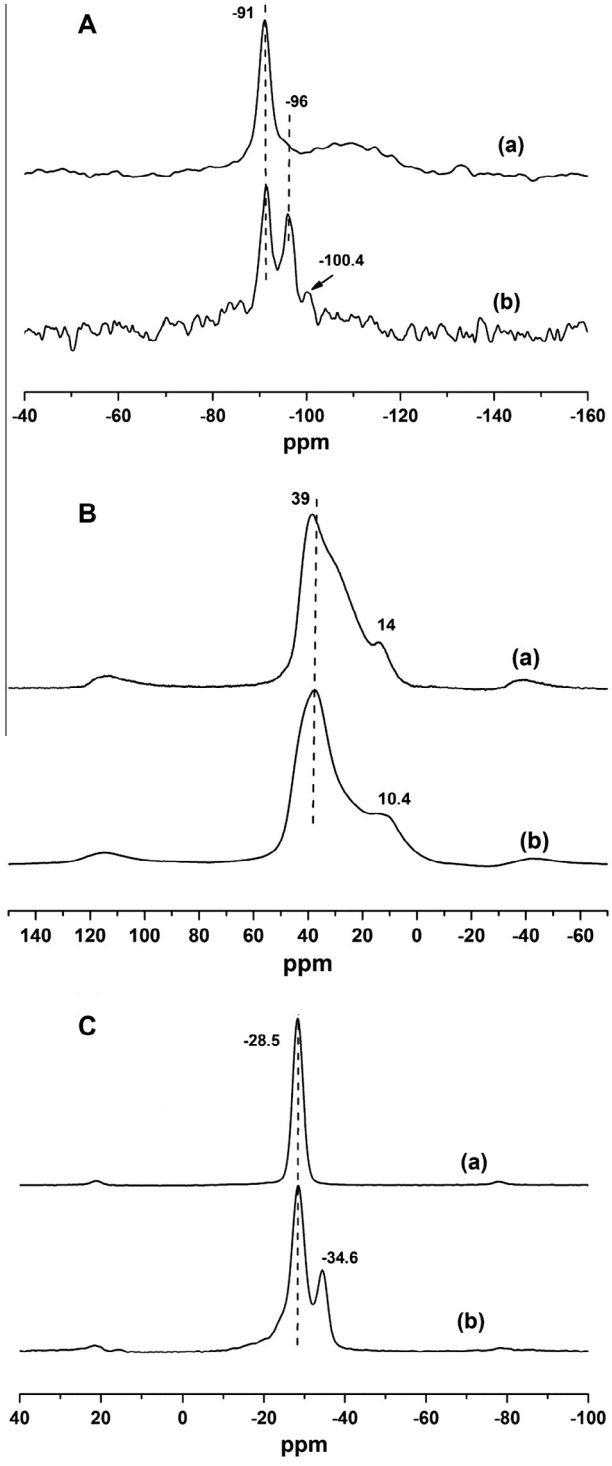

Fig. 6. ^{29}Si (A), ^{27}Al (B) and ^{31}P (C) MAS NMR spectra of the as-synthesized samples 4 (a) and 10 (b).

crystalline structure after calcination at 550 °C (Fig. S1 XRD and TG-DSC). For AlPO-22, although the structure is retained (Fig. S2 XRD and TG-DSC), the color of the sample becomes black. Further increasing the calcination temperature to 800 °C, the resulting sample shows a grayish color, suggesting the existence of some residual carbon. Given that AlPO-22 synthesized by other SDAs contains one phosphate group (HPO_4^{2-}) in each cavity of the framework [38,39], it is supposed that the phosphate group may also exist in the AlPO-22 templated by MDEA, which blocks the pore

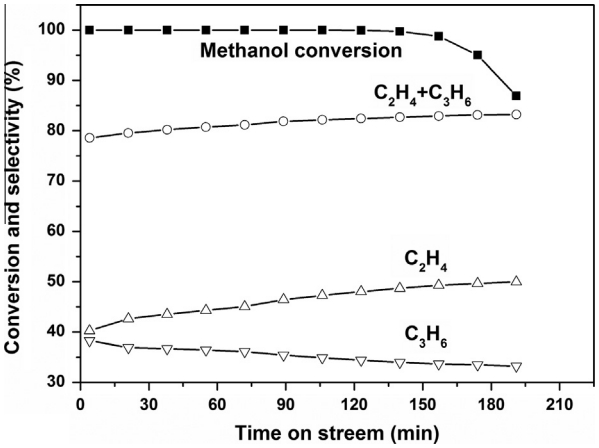

Fig. 7. Methanol conversion and selectivity of C_2H_4, C_3H_6 and C_2H_4 plus C_3H_6 during the MTO reaction on sample 3 (Reaction conditions: 450 °C, CH_3OH WHSV = 2 h^{-1}, N_2 as carrier gas).

and retards the removal of organics. Therefore, more attention has been paid to the physiochemical characterizations of SAPO-34 and SAPO-35.

The textural properties of SAPO-34 (sample 4) and SAPO-35 (sample 10) are characterized by nitrogen physical adsorption and the results are given in Table 2. SAPO-34 gives a BET surface area of 555 m^2/g and micropore volume of 0.27 cm^3/g. For SAPO-35, the BET surface area and micropore volume are 539 m^2/g and 0.24 cm^3/g respectively. These values are close to the reported, implying the good crystallinity of the two products.

The ^{13}C NMR spectra of the as-synthesized SAPO-34 and SAPO-35 are illustrated in Fig. 4. The spectra of the two samples show obvious chemical shifts and an increase in peak number and peak width as compared with the MDEA resource, suggesting the heterogeneous and distinct environments of MDEA in the cavities of both samples. It is supposed that flexible MDEA molecule adopts distinct molecular conformations in each material in order to match well with the pore structures. The much more splitting peaks in the spectra of SAPO-34 imply that the occluded MDEA may adopt at least two conformations. The electrostatic and van der Walls interactions between MDEA and the CHA frameworks arose different chemical shifts and broadness of the methyl and methylene carbon resonances. This finding is in agreement with the previous report that the conformations of amine in the molecular sieves are structure-dependent.

Fig. 5 shows the TG-DSC curves of the as-synthesized SAPO-34 and SAPO-35. The corresponding weight losses are summarized in Table 3. It is clear that the weight loss stages are different for both samples, which possibly result from the distinct existing status of the template, the microstructures and the acidity of the samples. The first endothermic weight loss (<210 °C for SAPO-34 and <300 °C for SAPO-35) is attributed to the desorption of water. Following the increase of the temperature, a three-stage exothermic weight loss in the range of 210–640 °C is observed for SAPO-34, which should be associated with the stepwise combustion decomposition of the template. SAPO-35 also gives a three-stage weight loss between 300 and 650 °C. But the removal of occluded template mainly occurred at higher temperature (>450 °C), suggesting the more stable environment of the template in the pores and cavities of SAPO-35. After 700 °C, no weight loss and exothermic peaks associated with structure collapse are observed until 800 °C, suggesting the good thermal stability of the two samples templated by MDEA.

Based on the elemental compositions and topological structures of SAPO-34 and SAPO-35, the average number of templates per

cage for the two samples was calculated, with the results of 1.54 MDEA for SAPO-34 and 1.05 MDEA for SAPO-35 (Table 3). The template number for SAPO-35 here is the same with the number of cyclohexylamine [40] and hexamethyleneimine [41] in the LEV cage. However, considering that MDEA has similar molecule size to triethylamine (TEA) and dipropylamine (DPA), it is quite interesting to see that the template number per CHA cage for MDEA is larger than that of the two alkylamines (one molecule per CHA cage). The reason for this phenomenon is possibly due to the higher polarity of alkanolamine as compared with that of alkylamines, which leads to a stronger interaction between alkanolamine–alkanolamine molecules and between the CHA framework and alkanolamine. The density of alkanolamine in each CHA cage can thus be increased. The much restricted space for MEDA in the CHA cage may cause its multiple conformations, consisting with the result of ^{13}C NMR spectrum.

Solid-state ^{29}Si, ^{27}Al and ^{31}P MAS-NMR spectra were determined to investigate the local environments of the as-synthesized SAPO-34 (sample 4) and SAPO-35 (sample 10). The results are shown in Fig. 6. The ^{29}Si spectrum of SAPO-34 shows one strong signal at −91 ppm, corresponding to the Si (4Al) environment. Additionally, there exists one weak peak at −96 ppm in the spectrum, which can be ascribed to the Si (3Al) environment. The ^{29}Si spectrum of SAPO-35 consists of two sharp peaks centered at −91 and −96 ppm and one weak peak at −100.4 ppm. According to the literatures [42,43], both strong resonances can be assigned to the Si(4Al) species in the framework of SAPO-35 with two different crystallographical T sites. The weak peak at −100.4 ppm possibly corresponds to the formation of 5Si islands in the framework. But an exact assignment of this resonance is difficult due to the existence of two T sites in the framework. ^{27}Al MAS NMR spectra of the two samples present one broad and asymmetric peak centered at 39 ppm accompanied with a weak one. The strong peak at high chemical shift should arise from the tetrahedrally coordinated aluminum atoms. The weak signals at around 14 ppm for sample 4 and 10 ppm for sample 10 are ascribed to the penta-coordinated Al formed by an additional interaction of one water or template molecule to the framework aluminum. Only one single resonance peak centered at −28.5 ppm is observed in the ^{31}P MAS NMR spectrum of SAPO-34, in accordance with P(4Al) environments. The ^{31}P spectrum of SAPO-35 consisted of two peaks centered at −28.5 and −34.6 ppm, which are attributed to the P_{T1}(4Al) and P_{T2}(4Al) species in the framework. The deconvoluted analysis of the spectrum shows that the two sites have a ratio of P_{T1}/P_{T2} = 1.90, close to the theoretical value of 2.

3.4. Catalytic performance in the MTO reaction

Considering the fact that SAPO-34 with lower Si contents generally exhibit better MTO performance [44,45]. Sample 3 was selected to test its catalytic properties in the MTO reaction. The results are illustrated in Fig. 7. It can be seen that the total selectivity of light olefins ($C_2H_4 + C_3H_6$) rises along with time and could reach the maximum of 82.7% under complete methanol conversion (TOS = 147 min). The selectivity of ethylene increases with time while the selectivity of propylene is just the opposite. The change of olefins selectivity with reaction time could attribute to the coking effect, which reduced the pore size of SAPO-34 and thus led to an increase of the ethylene/propylene ratio.

4. Conclusions

MDEA has been demonstrated to be a multifunctional template, which could direct the synthesis of six types of molecular sieves with pore sizes changing from 8- to 12-membered rings. Among these molecular sieves, SAPO-34, -35, AlPO-9 and -22 are for the first time obtained using MDEA template. The phase selectivity of the crystallization is sensitive to the synthetic gel compositions. SAPO-34 is acquired by the route of hydrothermal synthesis with relatively high concentration of MDEA in the initial gel, while the synthesis of SAPO-35 requires an aminothermal environment with a higher P_2O_5/Al_2O_3 ratio ($\geqslant 2$). AlPO-9 and -22 are obtained under the similar conditions to those of SAPO-35, except the absence of Si source. SAPO-34 and SAPO-35 templated by MDEA show good thermal stability, large pore volume and high surface area. The ^{13}C NMR spectra reveal that MDEA occluded in the final products keeps intact and adopts distinct molecular conformations to match with the pore structures (structure-dependent). A much condensed filling of MDEA is found in the CHA cage of SAPO-34 as compared with that of alkylamines, possibly due to the higher polarity of alkanolamine. The obtained SAPO-34 behaved good catalytic performance in the MTO reaction with a maximum of 82.7% light olefins ($C_2H_4 + C_3H_6$) selectivity under 100% methanol conversion.

Acknowledgment

We are grateful for the financial support from the National Natural Science Foundation of China (NSFC 21101150).

Appendix A. Supplementary material

Supplementary data associated with this article can be found, in the online version, at http://dx.doi.org/10.1016/j.jcis.2014.12.029

References

[1] S.T. Wilson, B.M. Lok, C.A. Messina, T.R. Cannan, E.M. Flanigen, J. Am. Chem. Soc. 104 (1982) 1146–1147.
[2] S.T. Wilson, B.M. Lok, E.M. Flanigen, U.S. Patent 4,310,440, 1982.
[3] Q. Huo, R. Xu, S. Li, Z. Ma, J.M. Thomas, R.H. Jones, A.M. Chippindale, J. Chem. Soc., Chem. Commun. (1992) 875
[4] Y. Wei, Z.J. Tian, H. Gies, R.R. Xu, H.J. Ma, R.Y. Pei, W.P. Zhang, Y.P. Xu, L. Wang, K.D. Li, B.C. Wang, G.D. Wen, L.W. Lin, Angew. Chem. Int. Ed. 49 (2010) 5367–5370.
[5] J.H. Yu, R.R. Xu, Accounts Chem. Res. 36 (2003) 481–490.
[6] B.M. Lok, C.A. Messina, R.L. Patton, R.T. Gajek, T.R. Cannan, E.M. Flanigen, J. Am. Chem. Soc. 106 (1984) 6092–6093.
[7] B.M. Lok, C.A. Messina, R.L. Patton, R.T. Gajek, T.R. Cannan, E.M. Flanigen, U. S. Patent 4, 440 (1984) 871.
[8] H.X. Liu, Z.K. Xie, C.F. Zhang, Q.L. Chen, Chin. J. Catal. 10 (2002) 49–54.
[9] M. Kang, J. Mol. Catal. A – Chem. 160 (2000) 437–444.
[10] P.-S.E. Dai, R.H. Petty, C.W. Ingram, R. Szostak, Appl. Catal. A 143 (1996) 101–110.
[11] R. Vomscheid, M. Briend, M.J. Peltre, P.P. Man, D. Barthomeuf, J. Phys. Chem. 98 (1994) 9614–9618.
[12] B.M. Lok, T.R. Cannan, C.A. Messina, Zeolites 3 (1983) 282–291.
[13] X.Q. Tong, J. Xu, C. Wang, W.F. Yan, J.H. Yu, F. Deng, R.R. Xu, Micropor. Mesopor. Mater. 183 (2014) 108–116.
[14] B. Zhang, J. Xu, F.T. Fan, Q. Guo, X.Q. Tong, W. Yan, J.H. Yu, F. Deng, C. Li, R.R. Xu, Micropor. Mesopor. Mater. 147 (2012) 212–221.
[15] X.Q. Tong, J. Xu, C. Wang, H.Y. Lu, P. Huang, W.F. Yan, J.H. Yu, F. Deng, R.R. Xu, Micropor. Mesopor. Mater. 155 (2012) 153–166.
[16] P. Huang, J. Xu, C. Wang, F. Deng, W.F. Yan, RSC Adv. 4 (2014) 39011–39019.
[17] D.W. Lewis, C.M. Freeman, C.R.A. Catlow, J. Phys. Chem. 99 (1995) 11194–11202.
[18] D.W. Lewis, C.R.A. Catlow, J.M. Thomas, Chem. Mater. 8 (1996) 1112–1118.
[19] D.W. Lewis, D.J. Willock, C.R.A. Catlow, J.M. Thomas, G.J. Hutchings, Nature 382 (1996) 604–606.
[20] B. Han, C.-H. Shin, P.A. Cox, S.B. Hong, J. Phys. Chem. B 110 (2006) 8188–8193.
[21] A.M. Prakash, S.V.V. Chilukuri, R.P. Bagwe, S. Ashtekar, D.K. Chakrabarty, Micropor. Mater. 6 (1996) 89–97.
[22] K.Y. Lee, H.-J. Chae, S.-Y. Jeong, G. Seo, Appl. Catal. A 369 (2009) 60–66.
[23] N. Rajić, D. Stojaković, S. Hoçevar, V. Kaučič, Zeolites 13 (1993) 384–387.
[24] E. Dumitriu, A. Azzouz, V. Hulea, D. Lutic, H. Kessler, Micropor. Mater. 10 (1997) 1–12.
[25] A.M. Prakash, S. Unnikrishnan, J. Chem. Soc., Faraday Trans. 90 (1994) 2291.
[26] L. Xu, A.P. Du, Y.X. Wei, Y.L. Wang, Z.X. Yu, Y.L. He, X.Z. Zhang, Z.M. Liu, Micropor. Mesopor. Mater. 115 (2008) 332–337.
[27] G.Y. Liu, P. Tian, Y. Zhang, J.Z. Li, L. Xu, S.H. Meng, Z.M. Liu, Micropor. Mesopor. Mater. 114 (2008) 416–423.
[28] G.Y. Liu, P. Tian, Z.M. Liu, Chin. J. Catal. 33 (2012) 174–182.

[29] L.P. Ye, F.H. Cao, W.Y. Ying, D.Y. Fang, Q.W. Sun, J. Porous Mater. 18 (2010) 225–232.
[30] Y.-J. Lee, S.-C. Baek, K.-W. Jun, Appl. Catal. A 329 (2007) 130–136.
[31] T. Ban, T. Ohwaki, Y. Ohya, Y. Takahashi, Int. J. Inorg. Mater. 1 (1999) 243–251.
[32] L. Chen, S.Y. Zhu, H.M. Wang, Y.M. Wang, Solid State Sci. 13 (2011) 2024–2029.
[33] D.H. Wang, P. Tian, M. Yang, S.T. Xu, D. Fan, X. Su, Y. Yang, C. Wang, Z.M. Liu, Micropor. Mesopor. Mater. 194 (2014) 8–14.
[34] D. Akolekar, S. Bhargava, J. Gorman, P. Paterson, Colloid. Surface A 146 (1999) 375–386.
[35] K.X. Wang, J.H. Yu, Z. Shi, P. Miao, W.F. Yan, R.R. Xu, J. Chem. Soc., Dalton Trans. (2001) 1809–1812
[36] W.F. Yan, J.H. Yu, Z. Shi, P. Miao, K.X. Wang, Y. Wang, R.R. Xu, Micropor. Mesopor. Mater. 50 (2001) 151–158.
[37] Y. Ding, N. Li, N.J. Guan, H.G. Wang, H.B. Song, S.H. Xiang, Micropor. Mesopor. Mater. 147 (2012) 68–72.
[38] J.W. Richardson Jr., J.J. Pluth, J.V. Smith, Naturwissenschaften 76 (1989) 467–469.
[39] W.F. Yan, J.H. Yu, R.R. Xu, G.S. Zhu, F.S. Xiao, Y. Han, K. Sugiyama, O. Terasaki, Chem. Mater. 12 (2000) 2517–2519.
[40] U. Lohse, F. Vogt, J. Richter-Mendau, Cryst. Res. Technol. 28 (1993) 1101–1107.
[41] N. Venkatathri, S.G. Hegde, P.R. Rajamohanan, S. Sivasanker, J. Chem. Soc., Faraday Trans. 93 (1997) 3411–3415.
[42] H.J. Jung, C.-H. Shin, S.B. Hong, J. Phys. Chem. B 109 (2005) 20847–20853.
[43] P. Tian, B. Li, S.T. Xu, X. Su, D.H. Wang, L. Zhang, D. Fan, Y. Qi, Z.M. Liu, J. Phys. Chem. C 117 (2013) 4048–4056.
[44] S. Wilson, P. Barger, Micropor. Mesopor. Mater. 29 (1999) 117–126.
[45] A. Izadbakhsh, F. Farhadi, F. Khorasheh, S. Sahebdelfar, M. Asadi, Y.Z. Feng, Appl. Catal. A 364 (2009) 48–56.